

## Theoretical resolution of the $H^-$ resonance spectrum up to the $n=4$ threshold. II. States of $^1S$ and $^1D$ symmetries

Miroslaw Bylicki<sup>1,\*</sup> and Cleanthes A. Nicolaides<sup>2,†</sup><sup>1</sup>*Instytut Fizyki, Uniwersytet Mikołaja Kopernika, Grudziądzka 5, 87-100 Toruń, Poland*<sup>2</sup>*Physics Department, National Technical University, Athens, and Theoretical and Physical Chemistry Institute, National Hellenic Research Foundation, 48 Vas. Constantinou Ave., 11635 Athens, Greece*

(Received 2 August 1999; revised manuscript received 12 October 1999; published 12 April 2000)

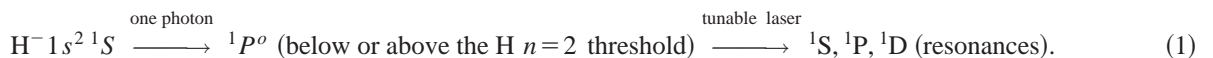
The resonance spectrum of  $H^-$  for  $^1S$  and  $^1D$  symmetries up to the  $n=4$  threshold has been computed by solving the corresponding complex eigenvalue Schrödinger equation in terms of basis functions of real and complex coordinates. These functions are chosen and optimized judiciously and systematically in order to account for the specific details of electronic structure, electron correlation, and multistate and multichannel couplings characterizing the problem. Large sets of Slater orbitals, extending in a regular manner to about 8000 atomic units, were employed in order to describe properly the full range and especially the large- $r$  behavior of the localized part of these resonances, as their energy approaches their corresponding threshold. Energies, widths, and wave-function characteristics are presented for 33  $^1S$  states and 37  $^1D$  states having widths down to about  $1 \times 10^{-9}$  a.u. Of this total of 70 states, only 32 have been identified before via the application of different theoretical approaches, or, for very few of them, in scattering experiments. By adopting the Gailitis-Damburg model of dipole resonances as the relevant zero order model, we identify unperturbed and perturbed spectral series, in analogy with the well-known spectra of neutral atoms or positive ions, where the zero-order model is based on the Rydberg spectrum of the  $1/r$  Coulomb potential. For perturbed spectra, only rough correspondence can be made with the smooth series predictions of the zero-order model. By achieving many-digit numerical precision for our results, we demonstrate the occasional presence of unique irregularities associated with each threshold, such as the existence of overlapping resonances and of “loner” resonances (i.e., not belonging to any series) below and above threshold. An example for the latter is a  $^1D$  shape resonance above the  $n=3$  threshold. This state was already identified by Ho and Bhatia [Phys. Rev. A **48**, 3720 (1993)]. However, our values for the energy above threshold ( $\Delta E=0.49497$  meV) and for the width ( $\Gamma=8.632$  meV) differ significantly from theirs ( $\Delta E=116.94$  meV and  $\Gamma=157$  meV).

PACS number(s): 31.50.+w, 32.80.Gc

### I. INTRODUCTION

This paper continues the presentation and the analysis of results on the resonance spectrum of the prototypical atomic negative ion,  $H^-$ , which started in our two concurrent papers [1,2], based on the solution of the complex eigenvalue Schrödinger equation for series of resonances. The symmetries of interest here are  $^1S$  and  $^1D$ , the energy range is from

the  $n=1$  to 4 hydrogen thresholds, and the adopted cutoff for the search of resonances are width values down to about  $1 \times 10^{-9}$  a.u. The above choices follow from the arguments presented in Ref. [2] as to the possibility of high resolution measurements of narrow  $H^-$  resonances of widths much smaller than 5–10 meV, via two-step excitation mechanisms. Accordingly, a possibly practical excitation path for the  $^1S$  and  $^1D$  resonances is



The  $^1P^o$  states around the  $n=2$  threshold have already been produced and measured below and above threshold at 10.172 and 10.226 eV above the H ground state respectively [3–7]. The even-parity states of  $^1P$  symmetry were calculated and analyzed in Ref. [1], for the energy spectrum up to

the  $n=5$  threshold and for widths down to about  $1 \times 10^{-10}$  a.u.

The implication of Eq. (1) is that the part of the  $^1S$  and  $^1D$  resonance spectra which were of immediate relevance to this work consists of the states which start above the  $n=2$  threshold. Nevertheless, for reasons of completeness and of comparison with the very recent results of Gien [8] for  $H^-$  resonances below the  $n=2$  threshold, we also give our results for the  $^1S$  and  $^1D$  resonances up to the  $n=2$  threshold and compare the positions and widths with his in Table I. In

\*Electronic address: mirekb@phys.uni.torun.pl

†Electronic address: can@eie.gr

TABLE I. Energies above the H ground state (in a.u.) and widths (in a.u.) of the  $^1S$  and  $^1D$  resonances below the  $n=2$  hydrogen threshold obtained from the solution of the complex eigenvalue Schrödinger equation (CESE, this work) and from the solution of the Harris-Nesbet algebraic coupled-channel equations (Gien, Ref. [8]). The notation  $[x]$  means  $10^{-x}$ .

	Gien [8]		This work	
	$E$	$\Gamma$	$E$	$\Gamma$
$^1S(1)$	0.351 232 565	1.736[3]	0.351 220 25	1.738 70[3]
(2)	0.373 990 251 35	8.93[5]	0.373 979 753	9.0934[9]
(3)	0.374 942 727 85	5.145[6]	0.374 942 173	5.2292[6]
(4)	0.374 996 717 2	2.943[7]	0.374 996 685 76	2.998[7]
(5)	0.374 999 811 85	1.6915[8]	0.374 999 809 851	1.7176[8]
(6)	0.374 999 992 1	6.34[10]	0.374 999 989	<4[9]
$^1D(1)$	0.372 099 877 05	3.153[4]	0.372 072 6	3.20[4]
(2)	0.374 999 670 3	2.462[8]	0.374 999 662 9	2.6[8]

Tables II and III we present our results for  $^1S$  and  $^1D$  resonances below the  $n=2$  threshold, including the distance from the nonrelativistic threshold,  $\epsilon_m$ , and the ratios for successive levels,  $R_\epsilon \equiv \epsilon_{m-1}/\epsilon_m$  and  $R_\Gamma \equiv \Gamma_{m-1}/\Gamma_m$ . Gien [8] employed the Harris-Nesbet algebraic method, and solved to high numerical accuracy the coupled-channel scattering (CCS) equations with 13 states. Given the reported number of significant digits, there is a discrepancy between these results and ours for the low-lying states. For these states, short-range correlation becomes relatively more important. We remind the reader that the energy region associated with the  $n=2$  threshold has been searched repeatedly since the early 1960s for the identification of resonances of different symmetries, computationally as well as experimentally (see Refs. [2–10], and references therein).

For the energy region of interest here, i.e., for the range between the  $n=2$  ( $-0.125$  a.u.) and  $n=4$  ( $-0.03125$  a.u.) hydrogen thresholds, the existing information since the 1960s concerns 11  $^1S$  and 13  $^1D$  resonances. The experimental and theoretical work is cited in Sec. II.

In the present calculations, we identified, analyzed, and classified 27  $^1S$  and 35  $^1D$  in the 2.5497 eV of this energy

range, with widths down to about  $1 \times 10^{-9}$  a.u. (As 1 a.u. for  $H^-$ , we use the reduced value 27.19658 eV.) The significance of these predictions, as well as of those in Refs. [1,2], is associated with the fundamentals of polyelectronic theory for resonance states, as well as with the possible future arrangements of experiments of high resolution (see Ref. [2]). They constitute the first very accurate resolution of a negative ion resonance spectrum over a physically reachable energy region, and provide reliable quantitative information about trends of spectral features of series of resonances and insight into their wavefunction characteristics.

## II. PREVIOUS DATA ON THE $E$ AND $\Gamma$ OF $H^-$ $^1S$ AND $^1D$ RESONANCES BETWEEN THE $n=2$ AND 4 THRESHOLDS

Simple calculations and their analysis show that configurations  $1snl, n \geq 2$ , do not lead to variationally optimized localized wave functions with energies in local-energy minima above the H  $1s$  energy at  $-0.5$  a.u. Therefore, no *shape* resonance associated with the  $n=1$  threshold exists.

It is at the  $n=2$  threshold that the structure of zero-order

TABLE II. Results of the present CESE (complex eigenvalue Schrödinger equation) calculations for  $H^-$  resonances of  $^1S^e$  symmetry below the  $n=2$  threshold.  $E$ : total energy in a.u. For  $H^-$ , 1 a.u.=27.19658 eV.  $\Gamma$ : total width.  $\epsilon_m \equiv E_{th} - E_m$ : the energy distance from threshold.  $R_\epsilon \equiv \epsilon_{m-1}/\epsilon_m$  and  $R_\Gamma \equiv \Gamma_{m-1}/\Gamma_m$ .

State	$-E$ (a.u.)	$\epsilon$ ( $10^{-8}$ a.u.)	$\frac{\Gamma}{2}$ ( $10^{-8}$ a.u.)	$R_\epsilon$	$R_\Gamma$
1	0.148 779 75	2 377 975		86 935	
2	0.126 020 247	102 024.7	4 546.7	23.31	19.12
3	0.125 057 827	5782.7	261.46	17.64	17.39
4	0.125 003 314 24	331.424	14.99	17.45	17.44
5	0.125 000 190 149	19.014 9	0.858 8	17.43	17.46
6	0.125 000 011	1.1	<0.2	17.3	<sup>a</sup>
The value of the ratio given by the GD model is [34]				17.429	

<sup>a</sup>Because of the extreme diffuseness of this state function and of the corresponding small number for  $\Gamma$ , the value for  $R_\Gamma$  did not have the same level of accuracy, and therefore it is excluded from the list.

TABLE III. As in Table II, for  ${}^1D^e H^-$  resonances below the  $n=2$  threshold.

State	$-E$ (a.u.)	$\epsilon$ ( $10^{-6}$ a.u.)	$\frac{\Gamma}{2}$ ( $10^{-6}$ a.u.)	$R_\epsilon$	$R_\Gamma$
1	0.127 927 4 <sup>a</sup>	2927.4	160.0		
2	0.125 000 337 1	0.3371	0.0130	8684.0	12307.0
The value of the ratio given by the GD model is [34]				4422	

<sup>a</sup>This energy corresponds to 10.8738 eV above the  $H^- {}^1S$  ground state, using 1 a.u. = 27.19658 eV and the nonrelativistic  $H^-$  energy  $-0.5277510$  a.u.. The two-photon experiment of Stintz *et al.* [35] gave  $10.872 \pm 0.002$  eV.

configurations allows localization, and hence the appearance of resonances below the  $n=2$  threshold such as “ $2s^2$ ”,  ${}^1S$ , “ $2p^2$ ”,  ${}^1D$ , etc. In fact, electron correlation also brings the  $2p^2 {}^3P$  state below the  $n=2$  threshold. Since the state does not mix with  $1s\epsilon l$  continua, it belongs to the discrete spectrum of  $H^-$ , together with the ground state  $1s^2 {}^1S$  [11]. *Ab initio* calculations have been used to conclude that no other discrete states of  $H^-$  exist [12]. The results presented in Tables I–III for  ${}^1S$  and  ${}^1D$  states, as well as in our other two papers [1,2] for other symmetries, show how close to the nonrelativistic  $n=2$  threshold there exist nonrelativistic complex eigenvalues. In Ref. [2] we commented on the possibility that one or more such eigenvalues might survive relativistic interactions, and therefore may correspond to *relativistic shape* resonances above the lowest relativistic  $n=2$  hydrogen threshold.

Resonances of  ${}^1S$  and  ${}^1D$  symmetries in the region between the  $n=2$  and 4 thresholds have attracted the interest of a number publications, which are briefly discussed below. On the experimental side, it is electron scattering experiments that have been carried out. The first measurement of the position (but not the width) of such states were made by McGowan and co-workers in the late 1960s [3]. They found one  ${}^1S$  state at 11.65 eV above H  $1s$ , and one  ${}^1D$  state at 11.89 eV. In the early 1970s, Spence [13] reported a measurement of the  $3p^2 {}^1D$  state at  $11.860 \pm 0.030$  eV. Years later, Williams [14], working with a resolution below 10 meV, identified two  ${}^1S$  and two  ${}^1D$  states below  $n=3$ . The positions as well as widths were measured. The same states were later detected by Warner, Rutter, and King [15], but only their energies were reported. The values of these energies are in slight disagreement with those of Williams. The above experimental data are presented in Table IV.

On the theoretical side, three categories of calculations

have been reported. The first is the variational diagonalization of the Feshbach-O’Malley-Geltman projected ( $QHQ$ ) real Hamiltonian in an  $\mathcal{L}^2$  basis of hydrogen and Slater functions by Oberoi [16]. This method produces only unshifted (by the interaction with open channels) energies and no width. In spite of this incomplete identification, at the time of their publication (1972) the Oberoi energies constituted a considerable advance in the knowledge of the whereabouts of five  ${}^1S$  states and four  ${}^1D$  states below  $n=3$ , and five  ${}^1S$  states and five  ${}^1D$  states below  $n=4$ . The second category is the diagonalization of non-Hermitian matrices to produce complex eigenvalues, the real part giving  $E$  and the imaginary one giving  $\Gamma$ . Two such methods have been applied. The first is the complex coordinate rotation (CCR) method, where the rotated Hamiltonian  $H(re^{-i\theta}) \equiv e^{-i2\theta}T + e^{-i\theta}V$  is diagonalized repeatedly as a function of  $\theta$  for one or more large  $\mathcal{L}^2$  basis sets, until a point of eigenvalue stability is recognized. The CCR method, as implemented and demonstrated by Doolen and co-workers [17,18], was applied to  $H^-$  in many publications starting in the late 1970s by Ho and co-workers [19–23], but only a few  ${}^1S$  and  ${}^1D$  resonances were identified. For example, below  $n=3$  only one  ${}^1S$  state [19] and one  ${}^1D$  state [20,22] have been reported. Also one  ${}^1D$  *shape* resonance above the  $n=3$  threshold was found [23]. Finally, below  $n=4$ , Ho [19] identified two  ${}^1S$  states, Ho and Callaway [20] two  ${}^1S$  states and three  ${}^1D$  states, and Ho [21] six  ${}^1S$  states. Our Tables V–VII contain the CCR results of Refs. [19–23].

The other method is that of solving the complex eigenvalue Schrödinger equation via the use of appropriate function spaces of real and complex coordinates. (See the discussion in Ref. [2].) Chrysos *et al.* [24] reported  $E$  and  $\Gamma$ , and also the partial widths with interchannel couplings for specific resonances of  ${}^1S$  symmetry (the lowest ones below the

TABLE IV. Experimental values for  $H^- {}^1S$  and  ${}^1D$  resonances between the  $n=2$  and 4 thresholds. The energies  $E$  are in eV above the H ground state, and the widths  $\Gamma$  are in meV.

	McGowan <i>et al.</i> [3] $E$	Spence [13] $E$	Williams [14] $E$ $\Gamma$		Warner <i>et al.</i> [15] $E$
${}^1S(1)$	$11.65 \pm 0.03$		11.723	$41 \pm 8$	$11.718 \pm 0.009$
${}^1S(2)$			12.026	$9 \pm 3$	$12.077 \pm 0.010$
${}^1D(1)$	$11.89 \pm 0.02$	$11.860 \pm 0.030$	11.805	$46 \pm 8$	$11.815 \pm 0.005$
${}^1D(2)$			12.04	$7 \pm 3$	$12.055 \pm 0.008$

TABLE V. Positions above the H ground state (in a.u.) and widths (in mau, 1 mau=10<sup>-3</sup> a.u.) of H<sup>-</sup> <sup>1</sup>S and <sup>1</sup>D resonances below the n=3 threshold, as identified in this and in previous works.

	Algebraic coupled channel Callaway [30]		<i>R</i> matrix Odgers <i>et al.</i> [32]		Ho [19]		Complex coordinate rotation				CESE This work	
	<i>E</i> (a.u.)	$\Gamma$ (mau)	<i>E</i> (a.u.)	$\Gamma$ (mau)	<i>E</i> (a.u.)	$\Gamma$ (mau)	Ho and Callaway [20]		Bhatia and Ho [22]		<i>E</i> (a.u.)	$\Gamma$ (mau)
							<i>E</i> (a.u.)	$\Gamma$ (mau)	<i>E</i> (a.u.)	$\Gamma$ (mau)		
<sup>1</sup> S(1)	0.431 003	1.430	0.431 00	1.52	0.431 00	1.42					0.430 993 94	1.417 86
(2)	0.442 232	0.306	0.442 28	0.299							0.442 218 27	0.308 22
(3)	0.443 872	0.0776	0.443 89	0.094							0.443 860 535	0.087 792
(4)	0.444 004	0.034	0.444 00	0.032							0.443 993 379	0.049 676
(5)											0.444 350 849 8	0.012 986
(6)											0.444 425 055 1	0.002 723 4
(7)											0.444 440 425 0	0.000 565 84
(8)											0.444 443 611 03	0.000 117 33
(9)											0.444 444 271 60	0.000 024 32
(10)											0.444 444 408 5	0.000 006 28
<sup>1</sup> D(1)	0.434 055	1.635	0.434 04	1.68			0.4340	1.6	0.434 046 7	1.658	0.434 041	1.652
(2)	0.443 188	0.242	0.443 21	0.242							0.443 169 4	0.2528
(3)	0.444 100	0.027	0.444 27	0.0214							0.444 241 73	0.041 68
(4)											0.444 266 13	0.049 36
(5)											0.444 411 505	0.006 856
(6)											0.444 439 084 0	0.001 123 2
(7)											0.444 442 533 9	0.000 781 4
(8)											0.444 443 570 62	0.000 183 112
(9)											0.444 444 301 97	0.000 029 6
(10)											0.444 444 420 6	0.000 011 4

TABLE VI. Positions above the H ground state (in a.u.) and widths (in mau, 1 mau =  $10^{-3}$  a.u.) of  $H^{-1}S$  and  $^1D$  resonances below the  $n=4$  threshold, as identified from the implementation of four methods for the calculation of resonances.

	R matrix		Complex coordinate rotation				Algebraic coupled channel		CESE	
	Pathak <i>et al.</i> [31]		Ho and Callaway [20]		Ho [21]		Callaway [30]		This work	
	$E$ (a.u.)	$\Gamma$ (mau)	$E$ (a.u.)	$\Gamma$ (mau)	$E$ (a.u.)	$\Gamma$ (mau)	$E$ (a.u.)	$\Gamma$ (mau)	$E$ (a.u.)	$\Gamma$ (mau)
$^1S(1)$	0.460 392	1.09	0.460 36	0.95	0.460 362	0.95	0.4603	1.0	0.460 364 71	0.954 66
(2)	0.465 307	0.71	0.465 27	0.88	0.465 27	0.88	0.4657	0.81	0.465 276 63	0.8636
(3)	0.466 475	0.27			0.466 433	0.34			0.466 433 30	0.340 36
(4)	0.468 005	0.093			0.467 982	0.127			0.467 982 66	0.127 954
(5)	0.468 483	0.045			0.468 491	0.046			0.468 493 13	0.045 34
(6)	0.468 540	0.045			0.468 53	0.07			0.468 531 196	0.069 572
(7)	0.468 662	0.013							0.468 664 27	0.015 208
(8)									0.468 721 274	0.005 134
(9)									0.468 736 113 1	0.004 744
(10)									0.468 740 36	0.001 720
(11)									0.468 746 766 3	0.000 561 4
(12)									0.468 748 916 1	0.000 195 48
(13)									0.468 749 144 14	0.000 292 76
(14)									0.468 749 637 3	0.000 065 04
(15)									0.468 749 880 4	0.000 020 2
(16)									0.468 749 947 20	0.000 018 34
(17)									0.468 749 98	0.000 02
$^1D(1)$	0.461 246	1.25	0.461 25	0.95			0.4613	1.2	0.461 263 6	0.9882
(2)	0.465 523	0.735	0.465 51	0.76					0.465 501 15	0.7674
(3)	0.466 829	0.210	0.466 87	0.24					0.466 838 2	0.3152
(4)	0.466 943	0.272							0.466 887 15	0.225 38
(5)	0.467 338	0.013							0.467 332 382	0.015 38
(6)	0.468 185	0.010							0.468 170 64	0.1098
(7)	0.468 475	0.0075							0.468 473 18	0.004 18
(8)	0.468 689	0.0075							0.468 569 8	0.052 86
(9)	0.468 696								0.468 569 80	0.035 506
(10)									0.468 694 66	0.000 76
(11)									0.468 693 77	0.011 24
(12)									0.468 732 598	0.003 50
(13)									0.468 738 816 5	0.000 254
(14)									0.468 740 005	0.003 328
(15)									0.468 742 142 5	0.001 916
(16)									0.468 744 565	0.001 084
(17)									0.468 747 742 4	0.000 032 0
(18)									0.468 748 299 4	0.000 337 4
(19)									0.468 749 467 4	0.000 106 6
(20)									0.468 749 502 28	0.000 151 78
(21)									0.468 749 545 19	0.000 008 76
(22)									0.468 749 836 7	0.000 039 0
(23)									0.468 749 911 5	0.000 002 86
(24)									0.468 749 979 7	0.000 012 66

$n=3$  and 4 thresholds.) The same quantities were reported by Themelis and Nicolaides [25] for  $^1D$  resonances below  $n=3$  and 4.

The third category consists of CCS calculations of different types, where fundamental quantities such as the phase shift or the reaction matrix are obtained as a function of real energy and then are used to fit appropriate formal expressions satisfied in the vicinity of a resonance. The first such

method to produce results for the resonances of interest was the direct numerical one, without and with correlation terms, implemented by Burke and collaborators in the 1960s [26–28]. They identified two  $^1S$  and  $^1D$  states below  $n=3$ . Callaway and coworkers [29,30] obtained algebraic solutions of the CCS equations using up to 28 states. Callaway identified four  $^1S$  states and three  $^1D$  states below  $n=3$ , and two  $^1S$  states and one  $^1D$  state below  $n=4$  [30]. Finally, the

TABLE VII. Energy (in  $10^{-4}$  eV above the H  $n=3$  threshold), width (in  $10^{-4}$  eV) and wave-function composition (in terms of the dominant symmetries) of the H<sup>-</sup>  $^1D$  shape resonance above the  $n=3$  threshold from the present CESE calculations. Comparison is made with  $E$  and  $\Gamma$  obtained by Ho and Bhatia [23], who implemented the CCR method.

CESE (this work)								CCR [23]	
$E$	$\Gamma$	$dd$	$sd$	$pp$	$pf$	$ff$	$dg$	$E$	$\Gamma$
4.965	8.6	0.561	0.234	0.092	0.084	0.017	0.012	1171	1569

$R$ -matrix method was applied by Pathak, Kingston, and Berrington [31] and Odgers, Scott and Burke [32]. Below the  $n=3$  threshold, four  $^1S$  states and three  $^1D$  states were identified [31,32], and below the  $n=4$  threshold seven  $^1S$  states and nine  $^1D$  states were found [31]. These results are included in Tables V and VI.

### III. PRESENT CALCULATIONS AND RESULTS

The theory and methodology which were applied for the present calculations were explained in the preceding paper [2]. Here we only discuss the implementation and the results.

The hydrogen states associated with the open channels, up to  $n=4$ , were represented by real Slater type orbitals (STO's) whose exponents were chosen equal to  $1/n$  so that, when combined, they can form the exact hydrogen functions. The real STO's used for the description of the localized parts of the wave functions as well as those complex STO's describing the outgoing Gamow orbitals, were chosen so that their average  $r$  values formed geometrical sequence covering the region from  $\langle r \rangle_{min}$  to  $\langle r \rangle_{max}$ . The values of  $\langle r \rangle_{min}$  and  $\langle r \rangle_{max}$  are given in Table VIII together with the number of localized STO's,  $N_{loc}$ , and complex rotated STO's,  $N_{rot}$ , for each orbital symmetry,  $l$ . The rotated orbitals were combined with the STO's representing the hydrogen target states to form the two-electron configurations describing the asymptotic part of the wave function. Since in the H<sup>-</sup> dipole resonances one electron is supposed to be, on average, close to the nucleus, whereas the other one moves in very large orbits, the whole orbital basis set was used for the outer electron and only half of it (the low  $\langle r \rangle$  part) was used for the inner electron. The number of configurations obtained in this way is given in Table IX together with the specification of angular  $ll'$  terms. The non-Hermitian Hamiltonian matrices were built from such bases, and diagonalized for 12 values of  $\theta$  in the range from 0.2 up to 0.75 rad. The  $\langle r \rangle_{min}$

TABLE IX. The basis set expansion for the CESE computation of  $^1S$  and  $^1D$  resonances. For a given total symmetry the number of radial terms within the angular contribution  $ll'$  is given.

	$ss$	$pp$	$dd$	$ff$	$gg$	$hh$	$sd$	$pf$	$dg$	$fh$	$gi$	Total
$^1S$	596	491	424	392	345	301						2549
$^1D$		436	373	343	299		884	759	655	582	501	4832

parameter was also optimized within a range of a few atomic units in order to obtain the best  $\theta$  stabilization of the complex roots corresponding to the sought after resonances. (The values of  $\langle r \rangle_{min}$  given in Table VIII define the lowest limit for this range.)

Our final results for the positions and widths of the  $^1S$  and  $^1D$  resonances are presented in Tables I, V, and VI, where they are compared with results of the most accurate and extensive previous calculations. We give the decimal figures which were found to be stable against variation of  $\theta$ .

The completeness of the present results as regards the resolution of the resonance spectra allow the possibility of analysis of general properties of the H<sup>-</sup> spectrum and of the resonance wave functions. Tables II, III, and X–XIII reveal the regularities and the disturbances of the resonance spectra. Specifically, apart from the energies and widths, we give the energy positions with respect to the threshold where the spectrum accumulates,  $\epsilon_m \equiv E_{th} - E_m$ , their ratio  $R_\epsilon \equiv \epsilon_{m-1}/\epsilon_m$ , and the ratio of the resonance widths,  $R_\Gamma \equiv \Gamma_{m-1}/\Gamma_m$ . Given the prediction of the dipole approximation [33], we classified the computed complex eigenvalues into series according to these ratios. According to the Gailitis-Damburg (GD) model [33], the ratios  $R_\epsilon$  and  $R_\Gamma$  should be the same for a given series. The model values of this ratio, obtained by Pathak, Burke, and Berrington [34], are also given in Tables II, III, and X–XIII.

If there is only one series in a given region, the convergence of ratios to the model value is quite good. Single series are predicted by the model [34] for  $^1D$  below the  $n=2$  threshold and for  $^1S$  below  $n=2$  and 3 thresholds. Let us consider the  $^1S$  series below the  $n=3$  threshold. Nine members of it have been identified by our computation (Table X). There is very nice convergence of the  $R_\epsilon$  and  $R_\Gamma$  to the model value. As discussed in Ref. [2], it is typical in such a case for  $R_\epsilon$  to approach the model value monotonically from above, and for  $R_\Gamma$  to do so from below. This is due to the fact that the binding of lower-lying members of the series is in fact stronger than that predicted by the GD model. However, here there is a clearly seen disturbance, caused by the

TABLE VIII. The orbital basis set used in the present computation of  $^1S$  and  $^1D$  resonances. The number of localized radial STO's,  $N_{loc}$ , and the number of complex rotated radial STO's,  $N_{rot}$ , for each orbital symmetry  $l$  are given. The STO's are chosen systematically so as to have their average  $r$  fall in a regular way inside the range defined by  $\langle r \rangle_{min}$  and  $\langle r \rangle_{max}$ .

	$s$		$p$		$d$		$f$		$g$		$h$		$i$		$\langle r \rangle_{min}$ (a.u.)	$\langle r \rangle_{max}$ (a.u.)
	$N_{loc}$	$N_{rot}$														
$^1S$	32	34	32	33	32	32	32		30		28			1.5	8000	
$^1D$	31	32	31	31	31	30	31	29	29	28	27	25		1.1	5500	

TABLE X. As in Table II, for  $1S^e H^-$  resonances below the  $n=3$  threshold. Note that, apart from the series  $A$  predicted by the GD model [34], the  $B$  state appears, which is not predicted by the model.

State	$-E$ (a.u.)	$\epsilon$ ( $10^{-8}$ a.u.)	$\frac{\Gamma}{2}$ ( $10^{-8}$ a.u.)	$R_\epsilon$	$R_\Gamma$
1 $A1$	0.069 006 06	1 345 050	70 893		
2 $A2$	0.057 781 73	222 617	15 411	6.042	4.600
3 $B$	0.056 139 465	58390.9	4389.6		
4 $A3$	0.056 006 621	45106.5	2483.8	4.938	6.204
5 $A4$	0.055 649 150 2	9359.46	649.3	4.819	3.825
6 $A5$	0.055 574 944 9	1938.93	136.17	4.827	4.76
7 $A6$	0.055 559 575 0	401.94	28.292	4.824	4.813
8 $A7$	0.055 556 388 97	83.341	5.8665	4.823	4.823
9 $A8$	0.055 555 728 40	17.284	1.216	4.822	4.824
10 $A9$	0.055 555 591 5	3.59	0.314	4.81	<sup>a</sup>
The value of the ratio given by the GD model is [34]				4.823	

<sup>a</sup>See the footnote of Table II.

occurrence of a “loner” state, which we labeled  $B$ . This state, not predicted by the model, appears between the  $A2$  and  $A3$  states of the discussed series, and pushes the  $A3$  level up. This is recognized by analyzing the  $R_\epsilon$  values. Another effect is that the  $A3$  state is more stable against autoionization, as compared to what would be expected from the regular behavior of unperturbed series.

The situation becomes more complicated and interesting when, in a given region, there are two or more series of resonances of the same symmetry. Then the interseries interaction often results in the lower-lying states of higher series being pushed up. As a consequence, the convergence of

higher series has different character than that of the lowest one.

Coexistence of different series leads also to the appearance of overlapping resonances. The most complicated case investigated in this work is that involving the  $1D$  resonances below the  $n=4$  threshold (see Table XIII). Our computation identified 24 states, which are classified into four series ( $A$ ,  $B$ ,  $C$ , and  $D$ ), in accordance with the prediction of the GD model. Among them there are five pairs of overlapping resonances. Members of such pairs belong to different series, and their energy difference is comparable to the width of at least one state of the pair. The most striking case is the overlap-

TABLE XI. As in Table II, for  $1S^e H^-$  resonances below the  $n=4$  threshold. Note the existence of overlapping resonances  $A4$  and  $B2$ .

State	$-E$ (a.u.)	$\epsilon$ ( $10^{-8}$ a.u.)	$\frac{\Gamma}{2}$ ( $10^{-6}$ a.u.)	$A$		$B$	
				$R_\epsilon$	$R_\Gamma$	$R_\epsilon$	$R_\Gamma$
1 $A1$	0.039 635 29	838529	477.33				
2 $B1$	0.034 723 37	347337	431.8				
3 $A2$	0.033 566 70	231 670	170.18	3.619	2.805		
4 $A3$	0.032 017 34	767 34	63.977	3.019	2.660		
5 $A4$	0.031 506 87	256 87	22.67	2.987	2.822		
6 $B2$	0.031 468 804	218 80.4	34.786			15.874	12.413
7 $A5$	0.031 335 73	8573	7.604	2.996	2.981		
8 $A6$	0.031 278 726	2872.6	2.567	2.984	2.962		
9 $B3$	0.031 263 886 9	1388.69	2.372			15.756	14.665
10 $A7$	0.031 259 64	964	0.860	2.980	2.985		
11 $A8$	0.031 253 233 7	323.37	0.2807	2.981	3.064		
12 $A9$	0.031 251 083 9	108.39	0.097 74	2.983	2.872		
13 $B4$	0.031 250 855 86	85.586	0.146 38			16.226	16.204
14 $A10$	0.031 250 362 7	36.27	0.032 52	2.988	3.006		
15 $A11$	0.031 250 119 6	11.96	0.0101	3.033	3.220		
16 $B5$	0.031 250 052 80	5.280	0.00917			16.209	15.963
17 $A12$	0.031 250 02	2	0.01	<sup>a</sup>	<sup>a</sup>		
The values of the ratio given by the GD model are [34]				2.982		16.210	

<sup>a</sup>See the footnote of Table II.

TABLE XII. As in Table II, for  ${}^1D^e H^-$  resonances below the  $n=3$  threshold. Note the existence of overlapping resonances  $A3$  and  $B1$ .

State	$-E$ (a.u.)	$\epsilon$ ( $10^{-6}$ a.u.)	$\frac{\Gamma}{2}$ ( $10^{-6}$ a.u.)	A		B	
				$R_\epsilon$	$R_\Gamma$	$R_\epsilon$	$R_\Gamma$
1 $A1$	0.065 959	10403	826				
2 $A2$	0.056 830 6	1275.0	126.4	8.159	6.535		
3 $A3$	0.055 758 27	202.71	20.84	6.290	6.065		
4 $B1$	0.055 733 87	178.31	24.68				
5 $A4$	0.055 588 495	32.939	3.428	6.154	6.079		
6 $A5$	0.055 560 916 0	5.360 4	0.561 6	6.145	6.104		
7 $B2$	0.055 557 466 1	1.910 5	0.390 7			93.332	63.169
8 $A6$	0.055 556 429 38	0.873 82	0.091 556	6.134	6.134		
9 $A7$	0.055 555 698 03	0.142 47	0.014 8	6.133	6.186		
10 $B3$	0.055 555 579 4	0.023 8	0.005 7			80.125	68.544
The values of the ratio given by the GD model are [34]				6.134		80.552	

ping pair of  $B2$  and  $A4$  states. Within the  $10^{-7}$  a.u. accuracy obtained for the  $B2$  state, their energies do not differ, and their widths are about  $52 \times 10^{-6}$  and  $35 \times 10^{-6}$  a.u. We thus have a case for the two-electron Coulomb Hamiltonian where near perfect degeneracy of states seems to exist on the

real energy axis. However, we hasten to point out that the resonance spectrum occurs in the second Riemann sheet as complex energies. Therefore, the meaning of the degeneracy must be expanded, referring to both real and imaginary energies. Actually, when  $\theta$  trajectories are followed, i.e., the

TABLE XIII. As in Table II, for  ${}^1D^e H^-$  resonances below the  $n=4$  threshold. Note the existence of pairs of overlapping resonances:  $B2$  and  $A4$ ,  $D3$  and  $A5$ ,  $D4$  and  $B3$ ,  $B3$ , and  $C2$ , and  $B4$  and  $D6$ .

State	$-E$ (a.u.)	$\epsilon$ ( $10^{-6}$ a.u.)	$\frac{\Gamma}{2}$ ( $10^{-6}$ a.u.)	A		B		C		D	
				$R_\epsilon$	$R_\Gamma$	$R_\epsilon$	$R_\Gamma$	$R_\epsilon$	$R_\Gamma$	$R_\epsilon$	$R_\Gamma$
1 $A1$	0.038 736 4	7486.4	494.1								
2 $B1$	0.034 498 85	3248.85	383.7								
3 $A2$	0.033 161 8	1911.8	157.6	3.916	3.135						
4 $C1$	0.033 112 85	1862.85	112.69								
5 $D1$	0.032 667 618	1417.618	7.69								
6 $A3$	0.031 829 36	579.36	54.9	3.300	2.871						
7 $D2$	0.031 526 82	276.82	2.09							5.121	3.679
8 $B2$	0.031 430 2	180.2	26.43			18.029	14.518				
9 $A4$	0.031 430 20	180.20	17.753	3.215	3.092						
10 $D3$	0.031 305 34	55.34	0.38							5.002	5.500
11 $A5$	0.031 306 23	56.23	5.62	3.205	3.159						
12 $A6$	0.031 267 402	17.402	1.75	3.231	3.211						
13 $D4$	0.031 261 183 5	11.183 5	0.127							4.948	2.992
14 $B3$	0.031 259 995	9.995	1.664			18.029	15.883				
15 $C2$	0.031 257 857 5	7.857 5	0.958					237.079	117.630		
16 $A7$	0.031 255 435	5.435	0.542	3.202	3.229						
17 $D5$	0.031 252 257 6	2.257 6	0.016 0							4.954	7.938
18 $A8$	0.031 251 700 6	1.700 6	0.168 7	3.196	3.213						
19 $A9$	0.031 250 532 6	0.532 6	0.053 3	3.193	3.165						
20 $B4$	0.031 250 497 72	0.497 72	0.075 89			20.082	21.926				
21 $D6$	0.031 250 454 81	0.454 81	0.004 38							4.964	3.653
22 $A10$	0.031 250 163 3	0.163 3	0.019 5	3.261	2.733						
23 $D7$	0.031 250 088 5	0.088 5	0.001 43							5.139	3.063
24 $B5$	0.031 250 020 3	0.020 3	0.006 33			24.518	11.989				
The values of the ratio given by the GD model are [34]				3.197		18.777		3227		4.940	

TABLE XIV. Wave-function characteristics for the  $^1S$   $H^-$  resonances lying below the  $n=3$  threshold.  $\langle r_{out} \rangle$  is the estimate for the size of each state due to the outer electron, computed as the average of the distance of the outer electron from the center of mass (in a.u.).  $R_{(r)}$  is the ratio of consecutive values of  $\langle r_{out} \rangle$ . The notation  $[x]$  means  $10^{-x}$ .

State	$\langle r_{out} \rangle$	$R_{(r)}$	$ss$	$pp$	$dd$	$ff$	$gg$	$hh$
1 A1	20.10		0.512	0.443	0.045	0.3[3]	0.8[6]	0.5[7]
2 A2	44.92	2.235	0.465	0.467	0.068	0.2[3]	0.6[6]	0.2[7]
4 A3	100.4	2.235	0.429	0.468	0.107	0.2[2]	0.2[5]	0.2[6]
5 A4	228.8	2.279	0.416	0.486	0.099	0.4[4]	0.4[7]	0.3[8]
6 A5	507.1	2.216	0.409	0.488	0.103	0.7[5]	0.7[8]	0.4[9]
7 A6	1118	2.205	0.406	0.489	0.105	0.1[5]	0.1[8]	0.8[10]
8 A7	2461	2.201	0.404	0.489	0.106	0.3[6]	0.3[9]	0.2[10]
9 A8	5408	2.197	0.404	0.490	0.107	0.6[7]	0.6[10]	0.4[11]
10 A9	11680	2.160	0.403	0.492	0.106	0.1[7]	0.1[10]	0.7[12]
3 B	29.80		0.294	0.125	0.563	0.022	0.3[4]	0.3[5]

dependence of the resonance eigenvalue on the rotation parameter  $\theta$  is determined, the roots are never degenerate, and in the limit of  $\theta=0$ , where they lie on the real axis, they are different from each other.

The classification of resonances into series is also supported by the recognition of their electron correlation patterns [36]. We obtained their size due to the outer electron  $\langle r_{out} \rangle$ , computed as the average of the distance of the outer electron from the nucleus, and the angular term contributions to the resonance wave functions. Resonances belonging to a given series have common angular electron correlation patterns, i.e., different states have the same contributions from various angular terms to their wave functions. The size of states increases as energy increases along a series. Furthermore, the ratio  $R_{(r)} = \langle r_{out} \rangle_{m+1} / \langle r_{out} \rangle_m$  converges along a given series to a well-determined value, which is characteristic of the series.

As an example of the above, consider the  $^1S$  resonances below the  $n=3$  threshold. We give their wave-function characteristics in Table XIV [37]. Series A, which is the only one predicted by the model, is characterized by large contributions from the  $ss$  and  $pp$  angular terms. On the other hand, the perturbing  $B$  state is mainly determined by the  $dd$  angular wave. Moreover, the characteristic ratio for the increasing size of states along the series is about 2.2, so that the  $B$  state, which is more compact than the  $A2$  state below  $B$ , does not fit the series. A similar case of a loner state not belonging to any of the model series was also found in the preceding paper [2]. Such states are essentially “created” by strong correlation and exchange effects which are not taken into account by the dipole model.

#### IV. SYNOPSIS

Together with the results and conclusions of [1,2] for  $H^-$  resonances of  $^1P$ ,  $^1P^o$ ,  $^1D^o$ , and  $^1F^o$  symmetries, the present work on  $^1S$  and  $^1D$  resonances constitutes a comprehensive determination of the  $H^-$  resonance spectrum for an energy range which, on the one hand, is sufficient to allow

a thorough understanding of the physics, and, on the other hand, can be probed by sophisticated experiments of very high resolution, at least in principle.

The theory and methods that we presented and applied, here and in Refs. [1,2], allow a practical and quantitative treatment of series of resonances in other systems as well, with two or more electrons. The identification of resonances is done in the conceptual framework of decaying states rather than by solving scattering-type equations. The solution of the complex eigenvalue Schrödinger equation involves the use of trial functions consisting of two major parts, one optimized on the real energy axis using real basis sets with real coordinates, and the other optimized in the complex energy plane, together with the first part, using basis sets of both real and complex coordinates.

In the present special case of  $H^-$ , we chose Slater-type orbitals with “group-of-states-specific” properties as regards their extent and their average  $r$ . Thus the various STO basis sets covered ranges of about 1–8000 a.u., representing both compact, “valence”-type intrashell configurations, mostly relevant for the representation of possible shape resonances, and diffuse, up to extremely diffuse, intershell configurations, relevant for the representation of the “dipole resonances” below each threshold. The resolution of these  $H^-$  resonance spectra is characterized by a very high numerical accuracy, covering the energy continuum up to the  $n=4$  threshold and widths down to about  $10^{-9}$  a.u. A total of 70  $^1S$  and  $^1D$  states were uncovered, one of them being a shape resonance and a few of them strongly overlapping, providing ample quantitative information for series of resonances of a negative ion. This fact allowed the categorization of the  $H^-$  spectra into unperturbed and perturbed series with respect to the Gailitis-Damburg model of dipole resonances.

#### ACKNOWLEDGMENTS

Support to one of us (M.B.) from the National Technical University of Athens is gratefully acknowledged. This work was supported by the Polish Committee for Scientific Research (Grant No. KBN 2 PO3B 125 18).

- [1] M. Bylicki and C. A. Nicolaides, *J. Phys. B* **32**, L317 (1999).
- [2] M. Bylicki and C. A. Nicolaides, preceding paper, *Phys. Rev. A* **61**, 052508 (2000).
- [3] J. W. McGowan, *Phys. Rev.* **156**, 165 (1967); J. W. McGowan, J. F. Williams, and E. K. Curley, *ibid.* **180**, 132 (1969); S. Ormonde, J. McEwen, and J. W. McGowan, *Phys. Rev. Lett.* **22**, 1165 (1969).
- [4] J. F. Williams, in *Progress in Atomic Spectroscopy*, edited by W. Hanle and H. Kleinpoppen (Plenum Press, New York, 1979), p. 1031.
- [5] H. C. Bryant, B. D. Dieterle, J. B. Donahue, H. Sharifian, H. Tootoonchi, D. M. Wolfe, P. A. M. Gram, and M. A. Yates-Williams, *Phys. Rev. Lett.* **38**, 228 (1977).
- [6] D. W. MacArthur, K. B. Butterfield, D. A. Clark, J. B. Donahue, P. A. M. Gram, H. C. Bryant, C. J. Harvey, and G. Comtet, *Phys. Rev. A* **32**, 1921 (1985).
- [7] H. H. Andersen, P. Ballingw, P. Kristensen, U. V. Pedersen, S. A. Aseyev, V. V. Petrunin, and T. Andersen, *Phys. Rev. Lett.* **79**, 4770 (1997).
- [8] T. T. Gien, *J. Phys. B* **31**, L1001 (1998).
- [9] G. J. Schulz, *Rev. Mod. Phys.* **45**, 378 (1973).
- [10] S. J. Buckman and C. W. Clark, *Rev. Mod. Phys.* **66**, 539 (1994).
- [11] I. Midtdal, *Phys. Rev.* **138**, A1010 (1965).
- [12] D. R. Beck and C. A. Nicolaides, *Chem. Phys. Lett.* **59**, 525 (1978).
- [13] D. Spence, *J. Phys. B* **8**, L42 (1975).
- [14] J. F. Williams, *J. Phys. B* **21**, 2107 (1988).
- [15] C. D. Warner, P. M. Rutter, and G. C. King, *J. Phys. B* **23**, 93 (1990).
- [16] R. S. Oberoi, *J. Phys. B* **5**, 1120 (1972).
- [17] G. D. Doolen, J. Nuttal, and R. W. Stagat, *Phys. Rev. A* **10**, 1612 (1974).
- [18] G. D. Doolen, *J. Phys. B* **8**, 525 (1975); *Int. J. Quantum Chem.* **14**, 523 (1978).
- [19] Y. K. Ho, *J. Phys. B* **10**, L373 (1977); **12**, L543 (1979).
- [20] Y. K. Ho and J. Callaway, *Phys. Rev. A* **27**, 1887 (1983); **34**, 130 (1986).
- [21] Y. K. Ho, *J. Phys. B* **23**, L71 (1990).
- [22] A. K. Bhatia and Y. K. Ho, *Phys. Rev. A* **41**, 504 (1990); **50**, 4886 (1994).
- [23] Y. K. Ho and A. K. Bhatia, *Phys. Rev. A* **48**, 3720 (1993).
- [24] M. Chrysos, Y. Komninos, Th. Mercouris, and C. A. Nicolaides, *Phys. Rev. A* **42**, 2634 (1990).
- [25] S. I. Themelis and C. A. Nicolaides, *Phys. Rev. A* **49**, 596 (1994).
- [26] P. G. Burke, S. Ormonde, and W. Whitaker, *Proc. Phys. Soc. London* **92**, 319 (1967).
- [27] A. J. Taylor and P. G. Burke, *Proc. Phys. Soc. London* **92**, 336 (1967).
- [28] J. Macek and P. G. Burke, *Proc. Phys. Soc. London* **92**, 351 (1967).
- [29] L. A. Morgan, M. R. C. McDowell, and J. Callaway, *J. Phys. B* **10**, 3297 (1977).
- [30] J. Callaway, *Phys. Rev. A* **26**, 199 (1982); **37**, 3692 (1988).
- [31] A. Pathak, A. E. Kingston, and K. A. Berrington, *J. Phys. B* **21**, 2939 (1988).
- [32] B. R. Odgers, M. P. Scott, and P. G. Burke, *J. Phys. B* **28**, 2973 (1995).
- [33] M. Gailitis and R. Damburg, *Proc. Phys. Soc. London* **82**, 192 (1963).
- [34] A. Pathak, P. G. Burke, and K. A. Berrington, *J. Phys. B* **22**, 2759 (1989).
- [35] A. Stintz, X. M. Zhao, C. E. M. Strauss, W. B. Ingalls, G. A. Kyrala, D. J. Funk, and H. C. Bryant, *Phys. Rev. Lett.* **75**, 2924 (1995).
- [36] For the classification of two-electron states by using approximate quantum numbers, see D. R. Herrick and O. Sinanoğlu, *Phys. Rev. A* **11**, 97 (1975); S. I. Nikitin and V. N. Ostrovsky, *J. Phys. B* **9**, 3141 (1976); D. R. Herrick, M. E. Kellman, and R. D. Poliak, *Phys. Rev. A* **22**, 1517 (1980); C. D. Lin, *Adv. At. Mol. Phys.* **22**, 77 (1986); J. M. Rost and J. S. Briggs, *J. Phys. B* **24**, 4293 (1991); Y. Komninos, S. I. Themelis, M. Chrysos, and C. A. Nicolaides, *Int. J. Quantum Chem., Symp.* **27**, 399 (1993).
- [37] Tables containing the wave-function characteristics for all the states under consideration can be obtained from [ftp://ftp.phys.uni.torun.pl/pub/publications/ifiz/mirekb/H\\_/tab\\_II.ps](ftp://ftp.phys.uni.torun.pl/pub/publications/ifiz/mirekb/H_/tab_II.ps).